

Conjugated metallorganic macrocycles: opportunities for coordination-driven planarization of bidentate, pyridine-based ligands†

Cite this: *Dalton Trans.*, 2013, **42**, 948Danielle C. Hamm,^a Lindsey A. Braun,^a Alex N. Burazin,^a Amanda M. Gauthier,^a Kendra O. Ness,^a Casey E. Biebel,^a Jon S. Sauer,^a Robin Tanke,^a Bruce C. Noll,^b Eric Bosch^c and Nathan P. Bowling^{*a}

Two conjugated systems that can be constrained to planarity *via* metal coordination have been generated and their metal complexes studied. The potential for these architectures to be incorporated into metal-sensing arylene ethynylene/vinylene oligomers and polymers was probed by verifying that these ligands (1) bind strongly to Ag(I) and Pd(II) cations, and (2) that this event leads to complexes that are planar. Single crystal structures confirm that introduction of Ag(I) or Pd(II) cations enforces planarity in the newly formed macrocycles. Likewise, ¹H-NMR titration studies reveal stoichiometric binding of Pd(II) and strong binding of Ag(I) ($K_a(\text{Ligand } 1) = 1.3 \times 10^2 \text{ M}^{-1}$; $K_a(\text{Ligand } 2) = 5.4 \times 10^2 \text{ M}^{-1}$) for each conjugated ligand.

Received 21st August 2012,
Accepted 16th October 2012

DOI: 10.1039/c2dt31914d

www.rsc.org/dalton

Introduction

Extensive electron delocalization in oligomeric and polymeric conjugated organic molecules leads to electronic properties that are desirable for a number of applications such as photovoltaics,^{1–3} light-emitting diodes^{4–6} and organic transistors.^{7–9} One pitfall with conjugated structures is that electronic properties can differ considerably from what would be predicted with a two-dimensional depiction. Conformational effects in such oligomeric and polymeric structures can substantially perturb or enhance effective conjugation. The ability to understand and perhaps control the conformational effects of these structures is, therefore, paramount.

In appropriately designed molecules, metal cations can alter the electronics of an unsaturated structure by both restricting rotation and withdrawing electron density from the π -system. Three of the most studied conjugated ligands used for this purpose are the 2,2'-bipyridine,^{10–13} 1,2-bis(2'-pyridinylethynyl)benzene,^{14–17} and quinoline/quinoxaline-ethynylene based systems^{18,19} (Fig. 1). Metal complexation in each of

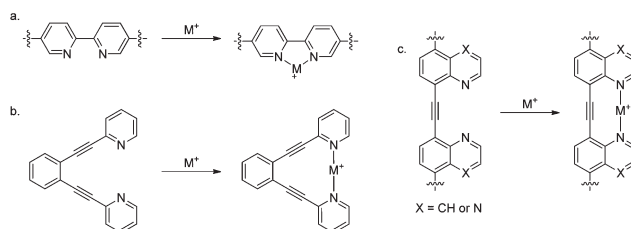


Fig. 1 Transition metal complexation to (a) 2,2'-bipyridines, (b) 1,2-bis(2'-pyridinylethynyl)benzenes and (c) quinoline/quinoxaline-ethynylenes enforces planarity in these conjugated systems.

these examples provides coordination-enforced planarity. This behavior can be used to alter the properties of conjugated oligomers/polymers in which these structures are incorporated²⁰ and in the development of transition metal sensors.²¹

1,2-Bis(2'-pyridinylethynyl)benzenes are a particularly interesting study in geometry. It is noted in a paper by Hu and co-workers¹⁵ that a palladium complex of this ligand is nearly “perfectly triangular with the C–C≡C–C (4.05 Å) and N–Pd–N (4.02 Å) distances being about equal.” With C–C≡C–C and N–Pd–N fragments acting as equivalently spaced building blocks, one can think of these metal complexes as equilateral “pseudo-dehydroannulene”²² triangles. With hopes of expanding the possibilities for coordination-driven planarization of conjugated molecules, we envisioned other unsaturated structures that might offer this same ability to be conformationally restricted upon introduction of a transition metal.

Arylethynyl ligand **1** and arylolefinyl ligand **2** (Fig. 2), should they be incorporated into larger oligomeric/polymeric

^aDepartment of Chemistry, University of Wisconsin-Stevens Point, 2001 Fourth Avenue, Stevens Point, WI 54481, USA. E-mail: nbowling@uwsp.edu

^bBruker AXS Inc., 5465 East Cheryl Parkway, Madison, WI 53711, USA

^cDepartment of Chemistry, Missouri State University, 901 S. National Ave., Springfield, MO 65897, USA

† Electronic supplementary information (ESI) available: ¹H NMR and ¹³C NMR spectra for all compounds, Ag(I) and Pd(II) titration data for **1** and **2**, and absorbance and fluorescence spectra for **1**, **2** and complexes are provided. CCDC 896707–896711. For ESI and crystallographic data in CIF or other electronic format see DOI: 10.1039/c2dt31914d

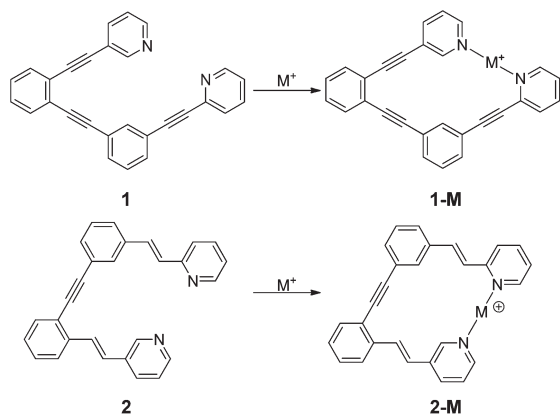


Fig. 2 Unsaturated ligands **1** and **2** have the appropriate alignment and spacing for bidentate binding of the pyridinyl rings to select transition metals. This binding event is predicted to enforce planarity in the conjugated backbone of the structure.

structures, could serve the same purpose as 2,2'-bipyridines, 1,2-bis(2'-pyridinylethynyl)benzenes and quinoxaline-ethynyls. That is, introduction of transition metal cations should enforce planarity, increasing the overall effective conjugation in these structures. Because of the similar C–C≡C–C and N–Pd–N distances noted above, **1-M** and **2-M** can be thought of as rhombus and parallelogram relatives, respectively, of the triangular 1,2-bis(2'-pyridinylethynyl)benzene metal complexes. Before incorporation of these structures into larger conjugated molecules, however, it must first be demonstrated (1) that **1** and **2** act as bidentate ligands for transition metals, and (2) that this binding event enforces coplanarity in the backbone.

Results and discussion

Electronic properties of **1** and **2** and their complexes

In a previous study, we have shown that introduction of transition metals to 1,2-bis(2'-pyridinylethynyl)benzene-based systems can lead to significant electronic changes in a conjugated backbone.²⁰ These types of changes likely require significant differences between the most favorable conformation of the ligand and the planar complex. While this can be achieved in longer conjugated systems, small, conjugated molecules such as ligand **1**, ligand **2**, and 1,2-bis(2'-pyridinylethynyl)benzene are unlikely to display dramatic, conformation-driven electronic shifts upon metal coordination. For these small molecules, the most favorable conformation likely involves coplanarity in the conjugated backbone. Any changes in conjugation upon metal complexation are therefore likely to be small.

Consistent with this expectation, 1,2-bis(2'-pyridinylethynyl)benzene shows only a small bathochromic shift in its absorption spectrum upon coordination to Pd(II).¹⁵ Similarly, dilute samples (8.2×10^{-6} M– 8.5×10^{-6} M in THF) of ligands **1** ($\lambda_{\text{max}} = 275$ nm, $\epsilon = 5.71 \times 10^4$ M⁻¹ cm⁻¹) and **2** ($\lambda_{\text{max}} = 277$ nm, $\epsilon = 5.89 \times 10^4$ M⁻¹ cm⁻¹) display only slight changes in molar

absorbance upon complexation to Ag(I) or Pd(II), with no significant spectral shifts in the absorption spectra. Absorbance spectra of Pd(II) complexes show small “tails” to the red of the major signals. These “tails” span into the visible region, giving the complexes a colored appearance. As has been observed for 1,2-bis(2'-pyridinylethynyl)benzene-based systems,²⁰ fluorescence in ligands **1** and **2** is quenched gradually with the addition of AgOTf and abruptly upon introduction of PdCl₂(PhCN)₂.

X-ray characterization of ligand

Ligands **1** and **2** are expected to have several low energy planar conformations that maximize conjugation while also minimizing repulsion between pyridyl non-bonding electron pairs. Single crystal X-ray diffraction studies, therefore, should reinforce electronic studies that suggest little conformational difference between ligand–metal complexes and the parent ligands. Thus, a crystal of ligand **1** was selected and the X-ray structure determined at –100 °C (crystals of ligand **2** suitable for X-ray analysis could not be obtained). Indeed the structure shown in Fig. 3A is essentially planar with the two pyridine rings mutually anti with respect to the central tolan moiety. The central phenyl rings are essentially coplanar with a torsional angle between them of approximately 3°. In contrast, the pyridyls are twisted with respect to the central tolan moiety in order to minimize the steric congestion between the hydrogens on the two pyridyl rings, specifically H4 and H26. The pyridyl–phenyl torsional angle is about 15°. The major crystal packing interaction in three dimensions is π -stacking with closest interactions between adjacent rings around 3.4 Å. The molecules are slip-stacked with a herringbone arrangement between adjacent columns of π -stacked molecules (shown in Fig. 3B and C) and one close C–H... π interaction of 2.743 Å between H11 and phenyl ring (C16–C21) that is shown by the dashed lines in Fig. 3B.

X-ray analysis of coordination complexes

Single crystal X-ray structural analysis was used to confirm the formation of the postulated planar rhombus and parallelogram shaped coordination complexes (Table 1 and 2). Accordingly, two coordination complexes of **1** were prepared and analyzed by single crystal X-ray diffraction. Thus a solution of the ligand **1** in dichloromethane was mixed with an acetonitrile solution containing 1 equiv. of silver(I) trifluoroacetate. After crystal formation appeared complete, a single crystal was cut for analysis and the structure was determined at –100 °C. The expected rhombus-shaped coordination complex was obtained as shown in Fig. 4A. The ligand is slightly bent and the tolan alkyne is not quite linear with bond angles C12–C14–C15 and C14–C15–C16 of 171.68 and 174.44° respectively. The pyridyl–silver–pyridyl bond is similarly slightly bent with bond angle N1–Ag1–N2 of 165.07°. The silver nitrogen bond distances of 2.188 and 2.197 Å are within the normal range.²³ There is a relatively strong monodentate interaction between the trifluoroacetate oxygen atom and the silver with a bond distance O1–Ag1 of 2.514 Å and angles O1–Ag1–N1 and

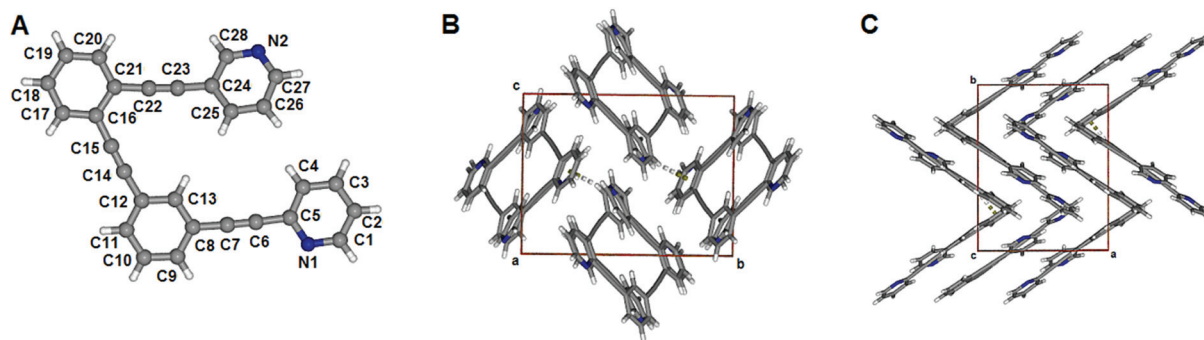


Fig. 3 (A) View of ligand **1** showing atom labeling. (B) Crystal packing of ligand **1** shown along the *a*-axis with the C–H– π interaction shown with dashed lines from the H to the centroid of the benzene ring. (C) As for (B) viewed along the *c*-axis showing the herringbone arrangement of adjacent stacks of the ligand.

Table 1 Crystal data for ligand **1** and coordination complexes of ligand **1**

	1	1 ·AgC ₂ F ₃ O ₂	1 ·PdCl ₂ ·CH ₂ Cl ₂
Formula	C ₂₈ H ₁₆ N ₂	C ₃₀ H ₁₆ AgF ₃ N ₂ O ₂	C ₂₉ H ₁₈ N ₂ PdCl ₄
<i>M</i> /g mol ^{−1}	380.43	601.32	642.65
Crystal system	Monoclinic	Monoclinic	Triclinic
Space group	<i>P</i> 2 ₁ / <i>c</i>	<i>P</i> 2 ₁ / <i>n</i>	<i>P</i> 1
<i>a</i> /Å	12.7773(14)	16.8364(17)	8.5163(5)
<i>b</i> /Å	14.4079(15)	7.9149(8)	11.2205(6)
<i>c</i> /Å	12.3216(13)	19.851(2)	14.9946(12)
α /°	90	90	102.112(1)
β /°	117.4760(10)	114.2540(10)	95.543(1)
γ /°	90	90	107.875(1)
<i>V</i> /Å ³	2012.5(4)	2411.8(4)	1313.21(15)
<i>Z</i>	4	4	2
$\rho_{\text{calcd.}}$ /g cm ^{−3}	1.256	1.656	1.625
μ /mm ^{−1}	1.061	0.891	1.136
<i>F</i> (0,0,0)	792	1200.0	640.0
Crystal size, mm	0.28 × 0.20 × 0.13	0.40 × 0.07 × 0.04	0.40 × 0.20 × 0.20
Temp./K	173(2)	173(2)	173(2)
θ range/°	1.8–27.2	1.3–27.2	1.4–27.2
Reflections collected	23 414	27 258	15 308
Independent reflections	4482	5356	5797
Data/restraints/parameters	4482/0/271	5356/0/343	5797/0/325
Goof	1.005	1.008	1.065
<i>R</i> (int)	0.058	0.088	0.014
Final <i>R</i> indices [<i>I</i> > 2 σ (<i>I</i>)], <i>R</i> ₁ / <i>wR</i> ₂	0.045/0.115	0.047/0.104	0.020/0.053
Largest diff. peak/hole/e Å ³	0.16/−0.18	0.83/−0.90	0.52/−0.68

O1–Ag1–N2 of 89.95 and 93.95° respectively. The slight butterfly effect is likely a manifestation of the crystal packing where the silver interacts weakly with the alkyne of the adjacent complex as shown in Fig. 4B to form discrete π -stacked pairs of the complex.²⁴ The pairs of complexes are then π -stacked in columns which have a herringbone-like arrangement between adjacent stacks as shown in Fig. 4C.

A palladium coordination complex was prepared in a similar way – a solution of the ligand **1** in dichloromethane was layered with a solution containing one equivalent of bis(acetonitrile) palladium(II) dichloride. Within several hours orange crystals started to form at the interface between the two

Table 2 Crystal data for coordination complexes of ligand **2**

	2 ·AgCF ₃ SO ₃ ·CH ₃ OH	2 ·PdCl ₂
Formula	C ₃₀ H ₂₄ AgF ₃ N ₂ O ₄ S	C ₂₈ H ₂₀ N ₂ PdCl ₂
<i>M</i> /g mol ^{−1}	673.45	561.76
Crystal system	Monoclinic	Orthorhombic
Space group	<i>P</i> 2 ₁ / <i>c</i>	<i>PF</i> ddd
<i>a</i> /Å	7.5430 (9)	16.0921(13)
<i>b</i> /Å	18.135 (2)	27.4790(13)
<i>c</i> /Å	20.575 (3)	44.234(3)
α /°	90	90
β /°	95.252 (4)	90
γ /°	90	90
<i>V</i> /Å ³	2802.7 (6)	19 560(2)
<i>Z</i>	4	32
$\rho_{\text{calcd.}}$ /g cm ^{−3}	1.656	1.526
μ /mm ^{−1}	0.85	0.996
<i>F</i> (0,0,0)	1360.0	9024.0
Crystal size, mm	0.60 × 0.10 × 0.06	0.29 × 0.20 × 0.05
Temp./K	200	173(2)
θ range/°	2.9–17.6	2.6–27.0
Reflections collected	43 347	55 436
Independent reflections	4958	5472
Data/restraints/parameters	4958/0/372	5472/0/298
Goof	1.046	1.087
<i>R</i> (int)	0.093	0.041
Final <i>R</i> indices [<i>I</i> > 2 σ (<i>I</i>)], <i>R</i> ₁ / <i>wR</i> ₂	0.041/0.104	0.026/0.068
Largest diff. peak/hole/e Å ³	0.59/−0.55	0.45/−0.32

solutions. After two weeks, large crystals had grown and a single crystal was selected for analysis. The structure of the discrete palladium complex, which includes a single dichloromethane solvent molecule, is shown in Fig. 5A. The palladium(II) atom has square planar coordination geometry with angles about palladium ranging from 87.66, 88.96, 90.22 and 93.12°. The N1–Pd1–N2 bond angle is 176.49° with palladium–nitrogen bond distances of 2.022 and 2.024 Å that are within the expected range.^{14,15} The overall structure is mostly planar, with torsional angles between pyridine and benzene rings of no more than 2° and a phenyl–phenyl angle of about 2.5°.

The chlorides of the palladium dichloride moiety are almost orthogonal to the essentially planar organic ligand and thereby preclude face-to-face π -stacking so the complexes are offset-stacked as shown in Fig. 5B and C.

Single crystals of ligand **2** with AgOTf were obtained by slow evaporation of a 2 : 1 methanol–dichloromethane mixture in

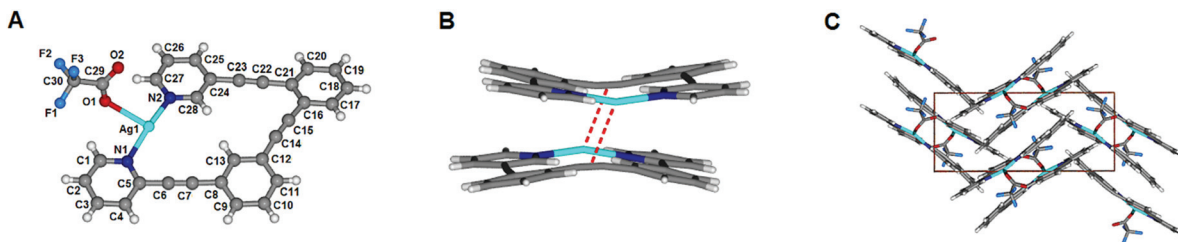


Fig. 4 (A) View of complex **1**-AgCF₃CO₂ showing atom labeling. (B) Side view of a pair of the coordination complexes with the weak silver–alkyne interaction shown with a dashed line from the silver to the centroid of the alkyne. (C) Crystal packing of the coordination complex viewed along the *a*-axis showing the herringbone arrangement of adjacent stacks of the complex.

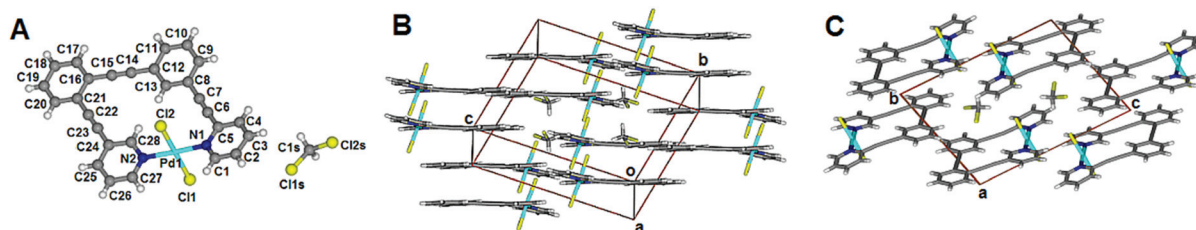


Fig. 5 (A) View of complex **1**-PdCl₂-CH₂Cl₂ showing the atom labeling. (B) Oblique view of the crystal packing showing the offset π -stacking of complexes. (C) View of the crystal packing along the *a*-axis.

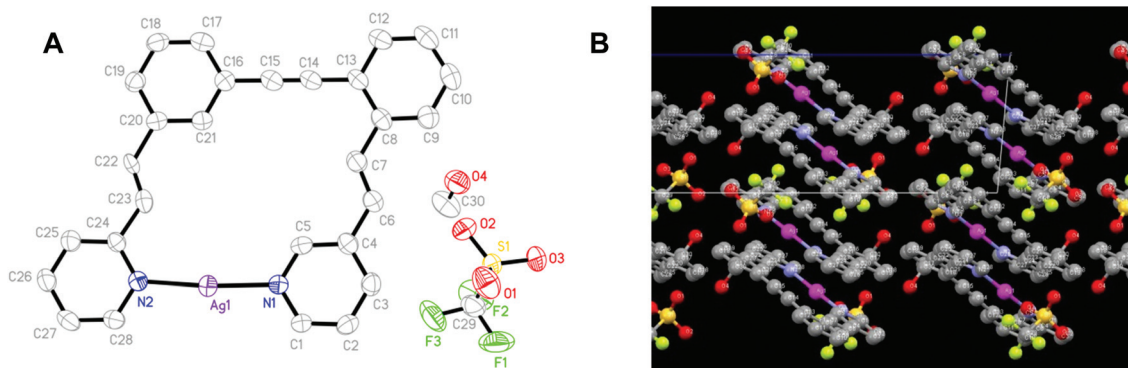


Fig. 6 (A) View of complex **2**-AgCF₃SO₃ showing the atom labeling. (B) Crystal packing of the coordination complex viewed along the *b*-axis showing a staggered arrangement of adjacent complexes.

the dark. A rod-shaped crystal was cut and placed into a sample holder, which was then cooled to -73 °C. As seen in Fig. 6A, the dipyrindyl ligand is essentially flat with all torsional angles deviating from planarity by less than 4.0° . The N1–Ag1–N2 bond angle (174.66°) and the Ag–N bond lengths (Ag1–N1: 2.127 Å, Ag1–N2: 2.141 Å) are close to what is expected for a two coordinate dipyrindyl silver complex.

The staggered orientation of the complex (Fig. 6B) is similar to what has been reported for the triangular complex.¹⁴ Trifluoromethanesulfonate anions and methanol molecules are located along the stacks of silver complexes with methanol forming a hydrogen bond with an oxygen atom of the triflate.

The complex of ligand **2** with palladium dichloride was formed and analyzed in a manner similar to complex **1**-PdCl₂. The coordination complex is planar with a torsional angle of approximately 3° between the benzene rings and about 1.4°

between each pyridyl ring and the phenyl ring it is connected to. The palladium has square planar geometry with palladium–nitrogen bond distances of 2.028 Å and 2.015 Å and bond angles about the palladium ranging from 88.38 to 91.54° . The N1–Pd1–N2 bond is 179.81° . The crystal packing involves π -stacking interactions with the orthogonal palladium dichloride moiety controlling the extent of overlap as shown in Fig. 7B and C.

NMR titration of ligands **1** and **2** with AgOTf and PdCl₂(PhCN)₂

It is clear from crystal structure analyses that ligands **1** and **2** form bidentate complexes with Ag(I) and Pd(II) in the solid state. To confirm this behavior in solution, NMR titration studies were performed. Introduction of small amounts of PdCl₂(PhCN)₂ led to a mixture of uncomplexed ligands **1** and **2**

and metal complexes **1-Pd** and **2-Pd**, respectively (Fig. 8). This complexation event was evidenced by significant downfield shifting of proton signals. The three signals for pyridine hydrogens at the 2 and 6 positions, for instance, are considerably downfield in complexes **1-Pd** and **2-Pd** from those of uncomplexed ligands **1** and **2** (Fig. 8). An additional two downfield signals found for **2-Pd** in this downfield region are tentatively assigned to intra-annular phenyl and vinyl hydrogens in the metallorganic macrocycle. Both ligands were found to bind stoichiometrically to Pd(II) in DMSO- d_6 with mixtures of unbound ligand and complex when less than one equivalent of Pd(II) is introduced, but no signal from unbound ligands at one equivalent Pd(II) or above. As expected for a system with 1 : 1 binding, no further changes are observed with additional PdCl₂(PhCN)₂.

In relation to Pd(II) studies, titrations with AgOTf were much less straightforward. Due to rapid complexation/

dissociation of the ligands and Ag(I) cations, separate ¹H NMR signals for complex and unbound ligand were not observed in DMSO- d_6 . Instead, increased levels of complexation were accompanied by gradual increases in chemical shifts (Fig. 9). Therefore, binding stoichiometry could not be ascertained *via* integration, but rather continuous variation Job plot analyses.^{25,26} To this end, a variety of solutions with different ligand : metal ratios, but a constant combined ligand + metal concentration (10.3 mM in DMSO- d_6), were analyzed *via* ¹H NMR spectroscopy. Plots of $\Delta\delta \times [\text{ligand}]$ vs. mole fraction Ag(I) reveal maxima at 0.5 mole fraction AgOTf, which is consistent with 1 : 1 binding ratios of ligand **1** and ligand **2** with the Ag(I) cation (Fig. 10).

As the primary motivation of this study is to generate conjugated frameworks that can be incorporated into functional organic materials and/or metal sensors, the binding strength of the ligands to the studied metals is of interest. As mentioned above, ligands **1** and **2**, like 1,2-bis(2'-pyridinylethynyl)-benzene, bind very efficiently to Pd(II) cations, even at high dilution. Because complexation to Ag(I) is dynamic on the NMR timescale, we anticipated this cation would provide a better platform for ligand comparison. At high concentration, complexation of these ligands to Ag(I) begins to approach stoichiometric binding. Consequently, titration experiments with our ligands had to be performed under very dilute conditions in order to achieve optimal equilibrium conditions. This high dilution was necessary to achieve an appropriate "p" value (actual concentration of complex/maximum possible concentration of complex) between 0.2 and 0.8, as defined by Weber.²⁷ Even at high dilution, samples that contained a large ratio of ligand to metal provided unreliable association

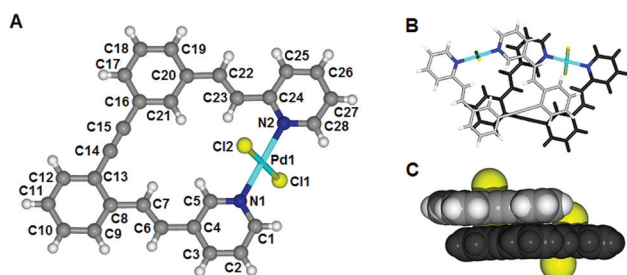


Fig. 7 (A) View of complex **2-PdCl₂** showing atom labeling. (B) View of offset π -stacking of two adjacent coordination complexes. (C) Side view of the two complexes in (B) with the atoms shown using the space filling option.

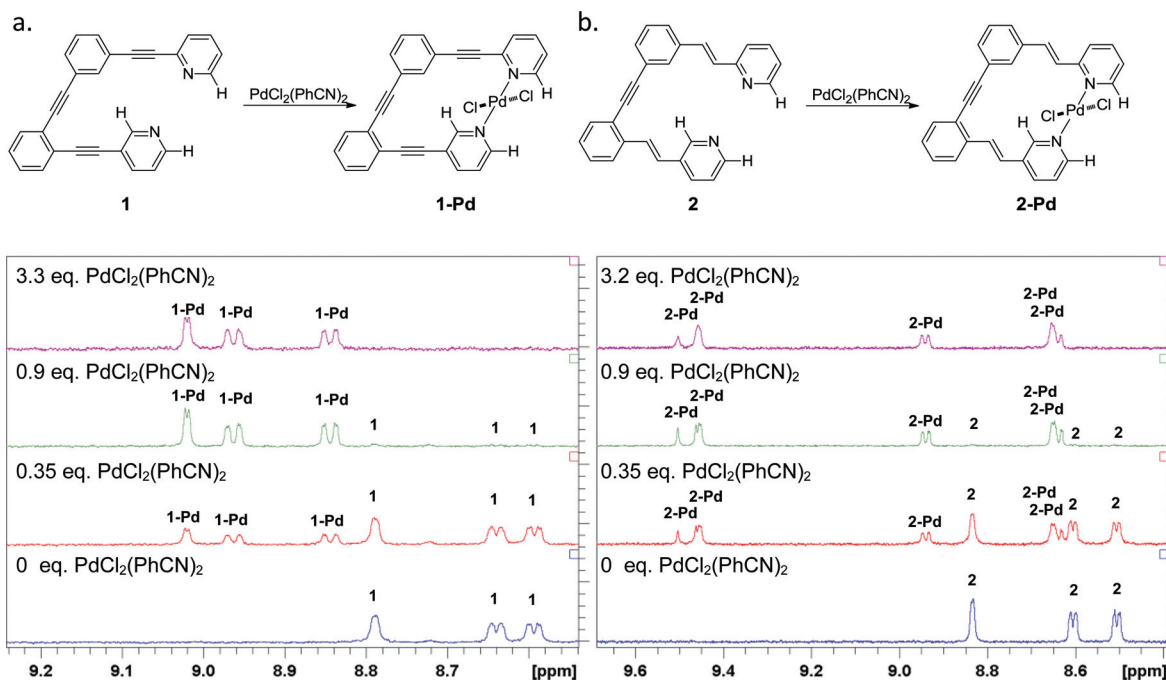


Fig. 8 Dilute samples in DMSO- d_6 (0.3–0.9 mM) with different mole fractions of PdCl₂(PhCN)₂ and (a) ligand **1** and (b) ligand **2** were studied *via* ¹H-NMR spectroscopy, revealing growth of signals corresponding to complexes **1-Pd** and **2-Pd** and diminishing signals for **1** and **2** upon addition of Pd(II).

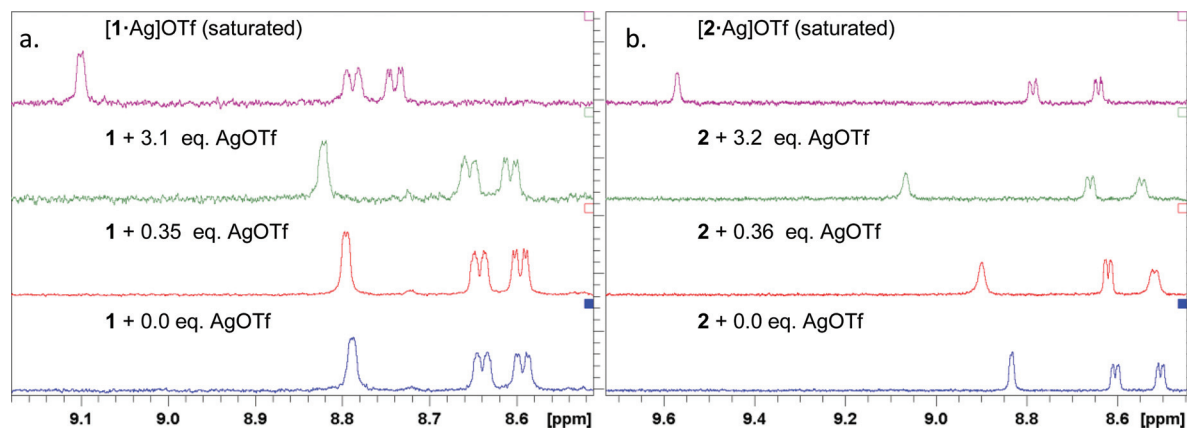


Fig. 9 Introduction of AgOTf to dilute solutions (0.28–0.88 mM) of ligands **1** and **2** in DMSO- d_6 leads to gradual downfield shifting of 2/6 pyridine hydrogen resonances in (a) ligand **1** and (b) ligand **2**.

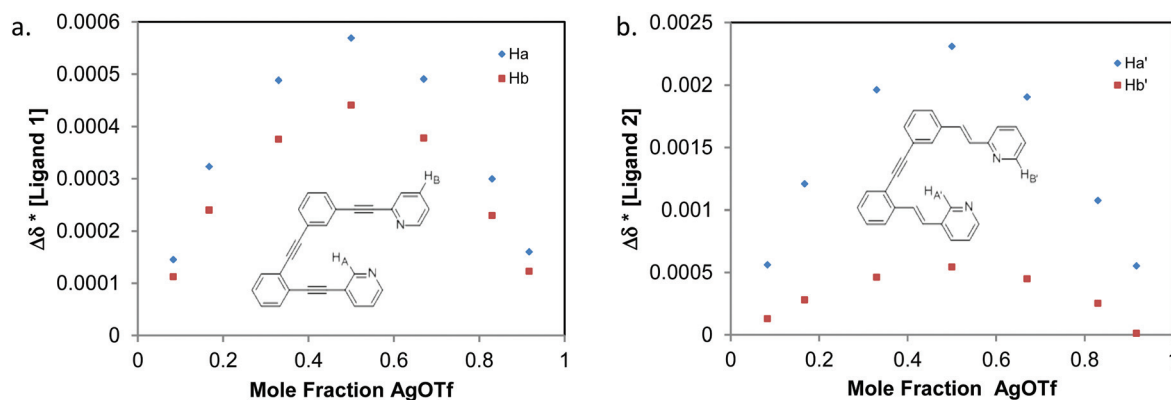


Fig. 10 Continuous variation Job plot analyses of ^1H NMR titration data (initial ligand concentrations of 1.7–9.5 mM in DMSO- d_6) confirm that (a) ligand **1** and (b) ligand **2** bind to Ag(I) cations with 1 : 1 stoichiometry.

constants. Once these limitations were identified, we were able to identify association constants with reproducibility.

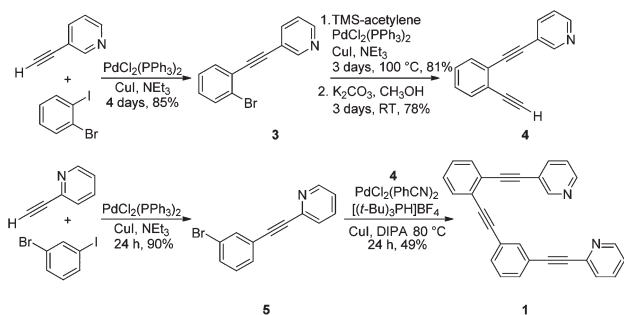
A variety of NMR samples containing different ratios of ligand to metal were made. Final concentrations of ligand **1** and ligand **2** ranged from 0.28 to 0.90 mM (in DMSO- d_6) and final Ag(I) concentrations ranged from 0.30 to 0.90 mM. The chemical shifts observed for these samples were compared to the chemical shifts of the free ligands (0.6 mM) and the totally saturated ligands (solid AgOTf added until no further changes in chemical shift were observed). The concentration of complex in each sample was calculated using the equation: $((\delta_{\text{obs}} - \delta_{\text{free}})/(\delta_{\text{sat}} - \delta_{\text{free}})) \times [\text{Ligand}]$, where δ_{obs} is the chemical shift observed for the equilibrating complex, δ_{free} is the chemical shift of the free ligand, and δ_{sat} is the chemical shift of the saturated system. With complex concentrations in hand, association constants could be calculated. Averaging all association constants obtained from different hydrogens and different trials, K values of $1.3 \times 10^2 \text{ M}^{-1}$ for ligand **1** and $5.4 \times 10^2 \text{ M}^{-1}$ for ligand **2** were obtained.

Comparing these ligands with each other and 1,2-bis(2'-pyridinylethynyl)benzene ($K = 1.3 \times 10^3 \text{ M}^{-1}$)²⁸ is instructive. It is not surprising that 1,2-bis(2'-pyridinylethynyl)benzene binds

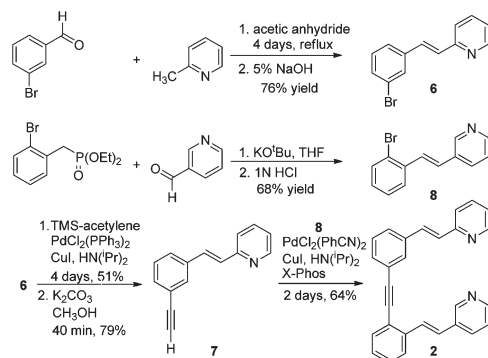
more tightly to the silver cation than ligands **1** and **2**, as complexation to the former requires restriction of fewer degrees of freedom. Differences between **1** and **2** are a little more surprising, however, as they possess very similar structures. We tentatively ascribe the stronger binding of **2** to electronic substituent effects. Based upon reported Hammett constants, styryl substituents can be slightly electron-donating to marginally electron-withdrawing.²⁹ Phenylethynyl substituents, on the other hand, are significantly more electron-withdrawing, likely decreasing the basicity of the pyridine lone pair, and therefore decreasing the binding constant. Steric hindrance between intra-annular hydrogen atoms could also destabilize a **1**-Ag⁺ complex. This interaction would be less problematic in the **2**-Ag⁺ complex, as the intra-annular hydrogens in this species are offset.

Ligand preparation

Ligand **1** was generated primarily *via* Sonogashira coupling reactions of commercially available haloarenes with commercially available ethynylpyridines (Scheme 1). 3-Ethynylpyridine is selectively coupled to the iodo position of 2-bromoiodobenzene upon treatment with appropriate catalysts to yield



Scheme 1 Generation of Ligand 1.



Scheme 2 Generation of Ligand 2.

compound 3. Under similar conditions, trimethylsilylacetylene is coupled to bromoarene 3. Removal of the trimethylsilyl protecting group can be achieved *via* treatment with a basic methanol solution, yielding 4. Sonogashira coupling of 2-ethynylpyridine with 1-bromo-3-iodobenzene at room temperature provides compound 5. Terminal alkyne 4 and bromoarene 5 can then be linked using coupling catalysts with electron-rich/sterically encumbered phosphine ligands at 80 °C, affording 1 in reasonable yields.

The condensation of 2-picoline with 3-bromobenzaldehyde in refluxing acetic anhydride offers the *trans* isomer of vinylpyridine 6 in high yields after basic workup. Alkene 8 is obtained in similarly high yields *via* Horner-Wadsworth-Emmons reaction of a phosphoester (obtained from 2-bromobenzylbromide) with 3-pyridinecarboxaldehyde. Linking these two isomers with an ethynyl group requires a familiar coupling-deprotection-coupling sequence, which gives ligand 2 in reasonable yields (Scheme 2).

Experimental

2-((3-((2-(Pyridin-3-ylethynyl)phenyl)ethynyl)phenyl)ethynyl)pyridine (1)

Bromoarene 5 (1.64 g, 6.37 mmol) was dissolved in a minimal amount of diisopropylamine and was transferred to a reaction vessel. PdCl₂(PhCN)₂ (0.128 g, 0.33 mmol), CuI (0.063 g, 0.33 mmol) and [(*t*-Bu)₃PH]BF₄ (0.096 g, 0.33 mmol) were

added and argon was bubbled through the mixture for 15 minutes. Terminal alkyne 4 (1.39 g, 6.85 mmol), dissolved in a minimal amount of diisopropylamine, was then added. After argon was bubbled through this mixture for 15 minutes, the vessel was sealed and heated at 80 °C for 24 hours. The resulting mixture was diluted with diethyl ether and the insoluble salts were removed *via* gravity filtration. The filtrate was washed with water, dried with anhydrous Na₂SO₄, filtered and concentrated under reduced pressure. The product was purified with consecutive applications of flash chromatography (1st: 1% EtOAc/99% ether, 2nd: 100% ether; both on silica gel). Appropriate fractions were concentrated to reveal product 1 as a white solid (1.19 g, 3.14 mmol, 49% yield, MP = 106–107 °C). ¹H-NMR (400 MHz, DMSO-*d*₆): δ = 8.82 (s, 1H), 8.68 (d, *J* = 4.2 Hz, 1H), 8.63 (d, *J* = 4.0 Hz, 1H), 8.04 (dt, *J* = 8.0, 1.9 Hz, 1H), 7.92 (td, *J* = 7.7, 1.8 Hz, 1H), 7.79 (m, 1H), 7.77–7.64 (m, 5H), 7.61–7.44 (m, 5H) ppm. ¹³C-NMR (100.6 MHz, DMSO-*d*₆): δ = 152.4, 151.1, 150.2, 142.9, 139.4, 137.7, 135.1, 133.0, 132.88, 132.86, 130.6, 130.3, 130.1, 128.5, 125.5, 125.2, 124.7, 123.7, 123.1, 120.1, 93.4, 91.7, 91.2, 90.6, 89.7, 87.9 ppm. ESI-MS (*m/z*) calcd for C₂₈H₁₆N₂H⁺ 381.1386; found 381.1401. λ_{max} nm (ε, M⁻¹ cm⁻¹) (THF) = 275 (57 100).

[1-Ag]OTf. ¹H-NMR (400 MHz, DMSO-*d*₆): δ = 9.10 (m, 1H), 8.79 (m, 1H), 8.74 (dd, *J* = 5.2, 1.4 Hz, 1H), 8.26 (dt, *J* = 8.0, 1.9 Hz, 1H), 8.14 (td, *J* = 8.0, 1.7 Hz), 7.96 (m, 2H), 7.75 (m, 6H), 7.57 (m, 3H) ppm. λ_{max} nm (ε, M⁻¹ cm⁻¹) (THF) = 273 (50 900), 300 (35 000).

1-PdCl₂. ¹H-NMR (400 MHz, DMSO-*d*₆): δ = 9.02 (d, *J* = 1.9 Hz, 1H), 8.96 (d, *J* = 5.7 Hz, 1H), 8.84 (d, *J* = 5.0 Hz, 1H), 8.30 (dt, *J* = 5.7, 1.6 Hz, 1H), 8.20 (t, *J* = 1.4 Hz, 1H), 8.07 (td, 7.8, 1.4 Hz, 1H), 7.89 (d, *J* = 7.2 Hz, 1H), 7.85 (m, 2H), 7.76 (m, 2H), 7.70 (m, 2H), 7.63 (m, 1H), 7.56 (m, 2H) ppm. λ_{max} nm (ε, M⁻¹ cm⁻¹) (THF) = 274 (67 600).

2-((E)-3-((2-((E)-2-(Pyridin-3-yl)vinyl)phenyl)ethynyl)styryl)pyridine (2)

Compound 8 (0.205 g, 0.778 mmol) was mixed with diisopropylamine (10 mL) under an argon atmosphere. CuI (0.0105 g, 0.055 mmol), X-Phos (0.0255 g, 0.053 mmol) and PdCl₂(PhCN)₂ (0.0208 g, 0.054 mmol) were added and argon was bubbled through the mixture for 15 minutes. Terminal alkyne 7 (0.245 g, 1.19 mmol) was added and the mixture was heated at 40 °C for two days. The mixture was rinsed into a flask with chloroform then concentrated under reduced pressure. The resulting residue was purified *via* flash chromatography (99% CH₂Cl₂/1% CH₃OH on silica gel). Appropriate fractions were concentrated to reveal the solid product (0.191 g, 0.497 mmol, 64% yield, MP = 136–137 °C). ¹H-NMR (400 MHz, CDCl₃): δ = 8.79 (s, 1H), 8.61 (d, *J* = 3.6 Hz, 1H), 8.51 (s, 1H), 7.86 (d, *J* = 7.9 Hz, 1H), 7.78 (d, *J* = 16.3 Hz, 1H), 7.77 (s, 1H), 7.70 (d, *J* = 7.9 Hz, 1H), 7.64 (td, *J* = 5.8, 1.7 Hz, 1H), 7.63 (d, *J* = 16.0 Hz, 1H), 7.58 (dd, *J* = 7.7, 1.2 Hz, 1H), 7.55 (d, *J* = 7.8 Hz, 1H), 7.48 (dt, *J* = 7.7, 1.3 Hz, 1H), 7.40–7.23 (m, 5H), 7.18 (d, *J* = 16.0 Hz, 1H), 7.16 (d, *J* = 16.6 Hz, 1H), 7.14 (m, 1H) ppm. ¹³C-NMR (100.6 MHz, CDCl₃): δ = 155.2, 149.7, 148.8, 148.7, 138.0, 137.0, 136.5, 133.1, 132.83, 132.76, 131.6, 131.1,

129.9, 128.91, 128.87, 128.75, 128.7, 127.8, 127.3, 126.6, 124.9, 123.7, 123.6, 122.4, 122.32, 122.27, 94.5, 87.9 ppm. ESI-MS (m/z) calcd for $C_{28}H_{20}N_2H^+$ 385.1705; found 385.1708. λ_{max} nm (ϵ , $M^{-1} cm^{-1}$) (THF) = 277 (58 900), 314 (54 800).

[2-Ag]OTf. 1H -NMR (400 MHz, DMSO- d_6): δ = 9.57 (m, 1H), 8.78 (d, J = 5.6 Hz, 1H), 8.64 (m, 1H), 8.43 (s, 1H), 8.25 (d, J = 8.4 Hz, 1H), 8.11 (m, 2H), 8.03 (d, J = 16.6 Hz, 1H), 7.99 (d, J = 7.8 Hz, 1H), 7.78 (m, 2H), 7.72 (m, 1H), 7.65 (d, J = 6.8 Hz, 1H), 7.63–7.47 (m, 6H), 7.42 (m, 1H) ppm. λ_{max} nm (ϵ , $M^{-1} cm^{-1}$) (THF) = 287 (63 900), 309 (53 500).

2-PdCl₂. 1H -NMR (400 MHz, DMSO- d_6): δ = 9.47 (d, J = 17.0 Hz, 1H), 9.45 (s, 1H), 8.94 (d, J = 5.3 Hz, 1H), 8.64 (m, 2H), 8.16 (d, J = 7.4 Hz, 1H), 8.13 (d, J = 16.5 Hz, 1H), 8.02 (m, 3H), 7.75 (d, J = 16.4 Hz, 1H), 7.66 (m, 2H), 7.60 (m, 3H), 7.55–7.41 (m, 4H) ppm. λ_{max} nm (ϵ , $M^{-1} cm^{-1}$) (THF) = 285 (61 300), 311 (46 400).

3-((2-Bromophenyl)ethynyl)pyridine (3)

PdCl₂(PPh₃)₂ (0.284 g, 0.40 mmol) and CuI (0.209 g, 1.10 mmol) were added to a reaction vessel. The tube was evacuated and purged with Ar ($\times 3$). Freshly distilled triethylamine (20 mL) was added, followed by 2-bromiodobenzene (0.91 mL, 7.07 mmol) and 3-ethynylpyridine (0.893 g, 8.66 mmol). The tube was sealed and the contents stirred for 4 days at room temperature. The resulting mixture was diluted with diethyl ether and gravity filtered. The filtrate was washed with water, dried with anhydrous Na₂SO₄, filtered and concentrated. This residue was purified *via* flash chromatography (25% EtOAc/75% hexanes on silica gel). The product was revealed as a yellowish oil (1.54 g, 5.98 mmol, 85% yield). 1H -NMR (400 MHz, CDCl₃): δ = 8.81 (dd, J = 2.8, 0.7 Hz, 1H), 8.56 (dd, J = 4.9, 1.7 Hz, 1H), 7.83 (dt, J = 7.9, 1.9 Hz, 1H), 7.61 (dd, J = 8.0, 1.1 Hz, 1H), 7.56 (dd, J = 7.7, 1.6 Hz, 1H), 7.29 (td, J = 7.6, 1.2 Hz, 1H), 7.27 (m, 1H), 7.19 (td, J = 7.8, 1.7 Hz, 1H) ppm. ^{13}C -NMR (100.6 MHz, CDCl₃): δ = 152.2, 148.9, 138.5, 133.3, 132.5, 129.9, 127.1, 125.6, 124.7, 123.0, 120.1, 91.1, 90.4 ppm. ESI-MS (m/z) calcd for C₁₃H₈⁷⁹BrNH⁺ 257.9913; found 257.9913.

3-((2-Ethynylphenyl)ethynyl)pyridine (4)

PdCl₂(PPh₃)₂ (0.218 g, 0.31 mmol) and CuI (0.057 g, 0.30 mmol) were added to a reaction vessel. The tube was evacuated and purged with Ar ($\times 3$). Bromoarene 3 (1.59 g, 6.18 mmol) was dissolved in freshly distilled triethylamine (20 mL) and transferred to the reaction vessel. Trimethylsilylacetylene (0.95 mL, 6.75 mmol) was added and the tube sealed and heated at 100 °C for three days. The resulting mixture was diluted with diethyl ether and gravity filtered. The filtrate was washed with water, dried with anhydrous Na₂SO₄, filtered and concentrated. The residue was purified *via* flash chromatography (5% EtOAc/95% hexanes on silica gel) revealing the TMS-protected product as a nearly colorless oil (1.37 g, 4.97 mmol, 81% yield). 1H -NMR (400 MHz, CDCl₃): δ = 8.80 (dd, J = 2.1, 0.8 Hz, 1H), 8.56 (dd, J = 4.9, 1.7 Hz, 1H), 7.82 (dt, J = 7.9, 1.9 Hz, 1H), 7.56–7.49 (m, 2H), 7.34–7.25 (m, 3H), 0.27 (s, 9H) ppm. ^{13}C -NMR (100.6 MHz, CDCl₃): δ = 152.3, 148.7,

138.4, 132.4, 131.8, 128.4, 128.3, 125.8, 125.3, 123.0, 120.5, 103.2, 99.0, 91.4, 89.8, 0.0 ppm. ESI-MS (m/z) calcd for C₁₈H₁₇NSiH⁺ 276.1203; found 276.1213. This oil was dissolved in a mixture of methanol (10 mL) and THF (10 mL). Enough K₂CO₃ was added to create a saturated solution and the reaction was stirred at room temperature for three days. Undissolved solid was removed *via* gravity filtration and the resulting mixture was flushed through a silica gel column with chloroform. Concentration of appropriate fractions revealed the product as a yellow solid (0.785 g, 3.86 mmol, 78% yield). 1H -NMR (400 MHz, CDCl₃): δ = 8.80 (dd, J = 2.1, 0.8 Hz, 1H), 8.56 (dd, J = 4.9, 1.7 Hz, 1H), 7.84 (dt, J = 8.0, 1.8 Hz, 1H), 7.56 (d, J = 2.0, 1H), 7.55 (d, J = 2.2 Hz, 1H), 7.39–7.27 (m, 3H), 3.38 (s, 1H) ppm. ^{13}C -NMR (100.6 MHz, CDCl₃): δ = 152.4, 148.8, 138.5, 132.7, 131.9, 128.6, 128.5, 125.6, 124.8, 123.0, 120.4, 91.0, 90.0, 82.0, 81.4 ppm. ESI-MS (m/z) calcd for C₁₅H₉NH⁺ 204.0808; found 204.0808.

2-((3-Bromophenyl)ethynyl)pyridine (5)

PdCl₂(PPh₃)₂ (0.249 g, 0.35 mmol) and CuI (0.082 g, 0.43 mmol) were added to a reaction vessel. The tube was evacuated and purged with Ar ($\times 3$). Freshly distilled triethylamine (20 mL) was added, followed by 3-bromiodobenzene (0.90 mL, 7.07 mmol) and 2-ethynylpyridine (0.79 mL, 7.78 mmol). The tube was sealed and the contents stirred for 24 hours. The resulting mixture was diluted with diethyl ether then gravity filtered to remove insoluble salts. The filtrate was washed with water, dried with anhydrous Na₂SO₄, filtered and concentrated under reduced pressure. The product was purified using flash chromatography (10% EtOAc/90% hexanes with slow increases in polarity, on silica gel). Appropriate fractions were concentrated to reveal the product as an off-white solid (1.64 g, 6.35 mmol, 90% yield). 1H -NMR (400 MHz, CDCl₃): δ = 8.62 (d, J = 4.8 Hz, 1H), 7.74 (t, J = 1.7 Hz, 1H), 7.67 (td, J = 7.7, 1.6 Hz, 1H), 7.50 (m, 3H), 7.22 (m, 2H) ppm. ^{13}C -NMR (100.6 MHz, CDCl₃): δ = 150.13, 143.0, 136.2, 134.7, 132.1, 130.5, 129.8, 127.2, 124.2, 123.0, 122.2, 89.8, 87.4 ppm. ESI-MS (m/z) calcd for C₁₃H₈⁷⁹BrNH⁺ 257.9913; found 257.9937.

(E)-2-(3-Bromostyryl)pyridine (6)

3-Bromobenzaldehyde (3.15 mL, 27.0 mmol), acetic anhydride (5.10 mL, 54.0 mmol) and 2-picoline (2.67 mL, 27.0 mmol) were refluxed in a 140 °C oil bath for one day. Another equivalent of 2-picoline (2.67 mL, 27.0 mmol) was added and the mixture was refluxed for another three days. Acetic anhydride was removed *via* distillation. While cooling with an ice bath, the reaction was quenched with water. 5% NaOH was added until the mixture was basic. The product was extracted with diethyl ether. This organic phase was washed with water, dried with anhydrous Na₂SO₄, filtered and concentrated under reduced pressure. The resulting residue was purified *via* flash chromatography (80% hexane/20% EtOAc, on silica gel). Appropriate fractions were concentrated to reveal the product as a yellow-brown solid (5.34 g, 20.5 mmol, 76% yield). 1H -NMR (400 MHz, CDCl₃): δ = 8.61 (d, J = 4.0 Hz, 1H), 7.72

(t, $J = 1.5$ Hz, 1H), 7.65 (td, $J = 7.7, 1.8$ Hz, 1H), 7.56 (d, $J = 16.0$ Hz, 1H), 7.46 (d, $J = 7.7$ Hz, 1H), 7.40 (d, $J = 7.9$ Hz, 1H), 7.35 (d, $J = 7.8$ Hz, 1H), 7.25 (d, $J = 8.2$ Hz, 1H), 7.21 (d, $J = 7.8$ Hz, 1H), 7.15 (m, 1H), 7.13 (d, $J = 16.0$ Hz, 1H) ppm. $^{13}\text{C-NMR}$ (100.6 MHz, CDCl_3): $\delta = 155.0, 149.7, 138.9, 136.6, 131.09, 131.06, 130.2, 129.7, 129.3, 125.8, 122.9, 122.44, 122.40$ ppm. ESI-MS (m/z) calcd for $\text{C}_{13}\text{H}_{10}^{79}\text{BrNH}^+$ 260.0075; found 260.0070.

(E)-2-(3-Ethynylstyryl)pyridine (7)

Compound **6** (1.13 g, 4.34 mmol) was mixed with diisopropylamine (10 mL) under an atmosphere of argon. To this was added $\text{PdCl}_2(\text{PPh}_3)_2$ (0.152 g, 0.22 mmol), CuI (0.058 g, 0.30 mmol), and another 10 mL diisopropylamine followed by trimethylsilylacetylene (0.61 mL, 4.3 mmol). This reaction mixture was heated at 80 °C for four days. The volatile contents were removed under reduced pressure. The remaining residue was dissolved in diethyl ether, washed with water ($\times 2$) and saturated NaCl solution, dried with anhydrous Na_2SO_4 , filtered and concentrated under reduced pressure. Purification was achieved *via* flash chromatography (70% hexane/30% EtOAc on silica gel). Appropriate fractions were concentrated to reveal the TMS-protected product as a beige solid (0.617 g, 2.22 mmol, 51% yield). $^1\text{H-NMR}$ (400 MHz, CDCl_3): $\delta = 8.59$ (d, $J = 4.7$ Hz, 1H), 7.70 (t, $J = 1.5$ Hz, 1H), 7.61 (td, $J = 7.7, 1.8$ Hz, 1H), 7.58 (d, $J = 16.0$ Hz, 1H), 7.47 (dt, $J = 7.7, 1.3$ Hz, 1H), 7.38 (dt, $J = 7.7, 1.3$ Hz, 1H), 7.32 (d, $J = 7.8$ Hz, 1H), 7.28 (t, $J = 7.7$ Hz, 1H), 7.14 (d, $J = 16.0$ Hz, 1H), 7.11 (ddd, $J = 7.4, 4.7, 1.0$ Hz, 1H), 0.27 (s, 9H) ppm. $^{13}\text{C-NMR}$ (100.6 MHz, CDCl_3): $\delta = 155.6, 150.0, 137.1, 136.8, 132.0, 131.9, 130.6, 129.0, 128.9, 127.7, 123.9, 122.6, 122.5, 105.2, 94.7, 0.3$ ppm. ESI-MS (m/z) calcd for $\text{C}_{18}\text{H}_{19}\text{NSiH}^+$ 278.1365; found 278.1364. Part of this solid (0.437 g, 1.58 mmol) was dissolved in equal parts methanol and THF. Enough K_2CO_3 was added to create a saturated solution and the reaction was monitored *via* TLC. After 40 minutes, the solvents were removed under reduced pressure. The residue was dissolved in diethyl ether, washed with brine and H_2O ($\times 2$), then was dried with anhydrous Na_2SO_4 , filtered and concentrated under reduced pressure. NMR spectroscopy revealed this product to be of sufficient purity (0.257 g, 1.25 mmol, 79% yield). $^1\text{H-NMR}$ (400 MHz, CDCl_3): $\delta = 8.59$ (d, $J = 4.0$ Hz, 1H), 7.69 (s, 1H), 7.61 (td, $J = 7.7, 1.8$ Hz, 1H), 7.58 (d, $J = 16.1$ Hz, 1H), 7.52 (d, $J = 7.8$ Hz, 1H), 7.40 (dt, $J = 7.7, 1.3$ Hz, 1H), 7.32 (d, $J = 7.8$ Hz, 1H), 7.30 (t, $J = 7.7$ Hz, 1H), 7.14 (d, $J = 16.1$ Hz, 1H), 7.11 (m, 1H), 3.11 (s, 1H) ppm. $^{13}\text{C-NMR}$ (100.6 MHz, CDCl_3): $\delta = 155.2, 149.7, 136.9, 136.5, 131.7, 131.5, 130.5, 128.8, 128.7, 127.5, 122.6, 122.3, 122.3, 83.4, 77.4$ ppm. ESI-MS (m/z) calcd for $\text{C}_{15}\text{H}_{11}\text{NH}^+$ 206.0970; found 206.0962.

2(E)-3-(2-Bromostyryl)pyridine (8)

2-Bromobenzyl bromide (5.00 g, 20.0 mmol) was converted to its corresponding phosphoester *via* dropwise addition of triethylphosphite (3.7 mL, 21.6 mmol) to a hot solution (100 °C) of the aryl halide solution in toluene (5 mL). After toluene was distilled off, the phosphoester was cooled and

diluted in anhydrous THF (7.5 mL). This solution was slowly added to a cold mixture (5 °C) of KO^tBu in THF (35 mL). At this temperature, a solution of pyridine-3-carboxaldehyde (2.07 mL, 22.1 mmol) in THF (5 mL) was added. After addition was complete, the resulting mixture was stirred for one hour at 0 °C. The reaction was quenched with 1 N HCl (40 mL). After separation of layers, the organic phase was washed with brine, dried with anhydrous Na_2SO_4 , filtered and concentrated under reduced pressure. The resulting residue was purified *via* flash chromatography (85% ether/15% hexane on silica gel). Appropriate fractions were concentrated to reveal the product (3.55 g, 13.6 mmol, 68% yield). $^1\text{H-NMR}$ (400 MHz, CDCl_3): $\delta = 8.71$ (d, $J = 1.6$ Hz, 1H), 8.50 (dd, $J = 4.7, 0.7$ Hz, 1H), 7.85 (dt, $J = 8.0, 1.7$ Hz, 1H), 7.64 (dd, $J = 3.8, 1.4$ Hz, 1H), 7.57 (dd, $J = 8.0, 0.8$ Hz, 1H), 7.50 (d, $J = 16.3$ Hz, 1H), 7.25–7.32 (m, 2H), 7.12 (td, $J = 7.7, 1.6$ Hz, 1H), 6.97 (d, $J = 16.3$ Hz, 1H) ppm. $^{13}\text{C-NMR}$ (100.6 MHz, CDCl_3): $\delta = 148.9, 148.8, 136.4, 133.1, 132.8, 132.6, 129.5, 129.3, 127.62, 127.56, 126.75, 124.2, 123.6$ ppm. ESI-MS (m/z) calcd for $\text{C}_{13}\text{H}_{10}\text{BrNH}^+$ 260.0075; found 260.0069.

Preparation of coordination complexes for X-ray analysis.

While ligands **1** and **2** are quite stable under standard atmospheric conditions, Ag(I) and Pd(II) complexes show slow discoloration upon extended exposure to air/light.

1-AgCF₃CO₂. A solution of **1** (21.0 mg, 0.055 mmol) in dichloromethane (2 mL) was mixed with a solution of silver(I) trifluoroacetate (12.1 mg, 0.055 mmol) in acetonitrile (2 mL). After two days, crystals started to form and the solvent was allowed to slowly evaporate until 1 mL of solvent remained. Clear rod-shaped crystals (30.7 mg, 92%) were isolated.

1-PdCl₂-CH₂Cl₂. A solution of bis(acetonitrile)palladium(II) dichloride (18.5 mg, 0.071 mmol) in acetonitrile (2 mL) was carefully layered over a solution of **1** (27.3 mg, 0.072 mmol) in dichloromethane (2 mL) and the solution allowed to stand. Block-shaped orange crystals started to form after several hours and, after standing for seven days, 39 mg (86%) of the product was isolated.

2-PdCl₂. A solution of bis(acetonitrile)palladium(II) dichloride (10.6 mg, 0.041 mmol) in acetonitrile (2 mL) was carefully layered over a solution of **2** (17.6 mg, 0.045 mmol) in dichloromethane (2 mL) and the solution allowed to stand. Trapezoidal orange crystals started to form after 16 hours and, after standing for seven days, 17 mg (74%) of the product was isolated.

2-AgOTf. To a solution of **2** (5.0 mg, 0.013 mmol) in methylene chloride was carefully added methanol (1 mL) followed by a solution of AgOTf (4.3 mg, 0.017 mmol) in methanol (1 mL). After approximately 10 days in the dark, single crystals were obtained by slow evaporation of the methanol-dichloromethane mixture. The crystals were rod shaped growing several hundred micrometers in length.

X-ray structure determination (1, 1-Ag, 1-Pd, 2-Pd). Crystals were mounted on a Kryolooop using viscous hydrocarbon oil. Data were collected using a Bruker Apex2 CCD diffractometer equipped with MoK α radiation with $\lambda = 0.71073$ Å. Data collection at low temperature, -100 °C, was facilitated by use of a Kryoflex system with an accuracy of ± 1 K. Initial data

processing was carried out using the Apex II software suite.³⁰ Structures were solved by direct methods using SHELXS-97 and refined using standard alternating least-squares cycles against F2 using SHELXL-97.³¹ The program X-Seed was used as a graphical interface.³² Hydrogen atoms were placed in idealized positions and refined with a riding model. Crystallographic details are summarized in ESI.† For complex 1·AgCF₃CO₂ the largest Q-peaks corresponded to a second minor conformation of the trifluoromethyl group and this disorder was not incorporated into the final solution given its low contribution. For complex 1·PdCl₂·CH₂Cl₂ the largest Q-peaks corresponded to a second minor position of the chlorides of the dichloromethane and this disorder was not incorporated into the final solution given its low contribution.

X-ray structure determination (2-Ag). A crystal was cut (0.60 × 0.10 × 0.06 mm) and placed quickly into the sample holder of a Bruker Benchtop SMART X2S (Bruker AXS, 2011). The sample in the instrument was cooled to −73 °C. Cell refinement and data reduction was completed using SAINT v7.68a (Bruker AXS, 2010). The structure was solved using SHELXS-97.³¹ Software used to prepare the structure for publication included the Apex II software suite³⁰ and PubCIF.³³ Full details are provided in the ESI.†

NMR titration studies/Job's plot analysis. Stock solutions of 1, 2, AgOTf and PdCl₂(PhCN)₂ were prepared by adding these solids to 5.00 mL volumetric flasks and diluting to mark with DMSO-d₆: ligand 1 (29.9 mg, 0.0786 mmol, 0.0157 M), ligand 2 (29.0 mg, 0.0754 mmol, 0.0151 M), AgOTf (20.9 mg, 0.0813 mmol, 0.0163 M), and PdCl₂(PhCN)₂ (27.5 mg, 0.0717 mmol, 0.0143 M). Into an NMR tube was added 10.0–30.0 μL of stock ligand solution followed by 10.0–30.0 μL of stock metal solution. These samples were diluted to a total volume of 540 μL (final concentration: 0.3–0.9 mM), mixed thoroughly (manual shaking of NMR tube), then analyzed *via* NMR spectroscopy. Metal solids were added to one sample until an endpoint was reached (*i.e.* no further changes in chemical shift were observed). *K* values were calculated by comparing chemical shifts of mixed samples with those of free ligands and the saturated sample.

UV-vis/fluorescence titration studies. Stock solutions of 1, 2, AgOTf and PdCl₂(PhCN)₂ were prepared by adding these solids to 5.00 mL volumetric flasks and diluting to mark with THF (HPLC grade): ligand 1 (16.2 mg, 0.0426 mmol, 8.52 mM), ligand 2 (17.6 mg, 0.0458 mmol, 9.16 mM), AgOTf (14.9 mg, 0.0580 mmol, 11.6 mM) and PdCl₂(PhCN)₂ (16.2 mg, 0.0422 mmol, 8.45 mM). Into 10.00 mL volumetric flasks was added 9.0–10.0 μL of stock ligand solution followed by 4.0–74.0 μL of stock metal solution. After dilution to mark with THF (final concentrations: 8.0–10.0 μM), these samples were analyzed *via* UV-vis and fluorescence spectroscopies.

Conclusions

Conjugated, organic ligands 1 and 2 bind Ag(I) and Pd(II) cations in a bidentate fashion. Coordination behavior of

these ligands has been confirmed *via* X-ray crystallography and ¹H-NMR spectroscopy. This binding event leads to metallorganic macrocycles that are constrained to planarity. While this coplanarity does not lead to major electronic changes in the parent systems studied, we anticipate that incorporation of these conjugated units into more elaborate structures will lead to unsaturated molecules with enhanced electronic properties and metal-ion sensing capabilities.

Acknowledgements

Acknowledgement is made to the donors of The American Chemical Society Petroleum Research Fund for support of this research. Additional support was provided by the Philip & Helen Marshall Chemistry Research Fund, the UWSP College of Letters and Sciences Undergraduate Education Initiative and the UWSP University Personnel Development Committee. NMR characterization was based upon work supported by the National Science Foundation under CHE-0957080. HR-MS characterization was based upon work supported by the National Science Foundation under CBET-0958711. The Missouri State University Provost Incentive Fund funded the purchase of the X-ray diffractometer.

References

- 1 A. W. Hains, Z. Q. Liang, M. A. Woodhouse and B. A. Gregg, *Chem. Rev.*, 2010, **110**, 6689.
- 2 S.-S. Sun and N. S. Sariciftci, *Organic Photovoltaics*, Taylor & Francis, Boca Raton, 2005.
- 3 S. Gunes, H. Neugebauer and N. S. Sariciftci, *Chem. Rev.*, 2007, **107**, 1324.
- 4 G. M. Farinola and R. Ragni, *Chem. Soc. Rev.*, 2011, **40**, 3467.
- 5 K. Mullen and U. Scherf, *Organic Light-Emitting Devices*, Wiley-VCH, Weinheim, 2006.
- 6 M. A. Baldo, D. F. O'Brien, Y. You, A. Shoustikov, S. Sibley, M. E. Thompson and S. R. Forrest, *Nature*, 1998, **395**, 151.
- 7 B. Lucas, T. Trigaud and C. Vidolot-Ackermann, *Polym. Int.*, 2012, **61**, 374.
- 8 A. R. Murphy and J. M. J. Frechet, *Chem. Rev.*, 2007, **107**, 1066.
- 9 C. Wang, H. Dong, W. Hu, Y. Liu and D. Zhu, *Chem. Rev.*, 2012, **112**, 2208.
- 10 A. Kokil, P. Yao and C. Weder, *Macromolecules*, 2005, **38**, 3800.
- 11 B. Wang and M. R. Wasielewski, *J. Am. Chem. Soc.*, 1997, **119**, 12.
- 12 K. D. Ley, Y. T. Li, J. V. Johnson, D. H. Powell and K. S. Schanze, *Chem. Commun.*, 1999, 1749.
- 13 M. Zhang, P. Lu, Y. G. Ma and J. C. Shen, *J. Phys. Chem. B*, 2003, **107**, 6535.
- 14 E. Bosch and C. L. Barnes, *Inorg. Chem.*, 2001, **40**, 3097.

- 15 Y. Z. Hu, C. Chamchoumis, J. S. Grebowicz and R. P. Thummel, *Inorg. Chem.*, 2002, **41**, 2296.
- 16 J. E. Fiscus, S. Shotwell, R. C. Layland, M. D. Smith, H. C. zur Loye and U. H. F. Bunz, *Chem. Commun.*, 2001, 2674.
- 17 T. Kawano, J. Kuwana, T. Shinomaru, C. X. Du and I. Ueda, *Chem. Lett.*, 2001, 1230.
- 18 Y. X. Xu, T. G. Zhan, X. Zhao, Q. A. Fang, X. K. Jiang and Z. T. Li, *Chem. Commun.*, 2011, **47**, 1524.
- 19 N. J. Greco, M. Hysell, J. R. Goldenberg, A. L. Rheingold and Y. Tor, *Dalton Trans.*, 2006, 2288.
- 20 Q. Ren, C. G. Reedy, E. A. Terrell, J. M. Wieting, R. W. Wagie, J. P. Asplin, L. M. Doyle, S. J. Long, M. T. Everard, J. S. Sauer, C. E. Baumgart, J. S. D'Acchioli and N. P. Bowling, *J. Org. Chem.*, 2012, **77**, 2571.
- 21 E. Bosch, C. L. Barnes, N. L. Brenrian, G. L. Eakins and B. E. Breyfogle, *J. Org. Chem.*, 2008, **73**, 3931.
- 22 S. Shotwell, H. L. Ricks, J. G. M. Morton, M. Laskoski, J. Fiscus, M. D. Smith, K. D. Shimizu, H. C. zur Loye and U. H. F. Bunz, *J. Organomet. Chem.*, 2003, **671**, 43.
- 23 C. Y. Chen, J. Y. Zeng and H. M. Lee, *Inorg. Chim. Acta*, 2007, **360**, 21.
- 24 C. Janiak, *J. Chem. Soc., Dalton Trans.*, 2000, 3885.
- 25 V. M. S. Gil and N. C. Oliveira, *J. Chem. Educ.*, 1990, **67**, 473.
- 26 J. T. Sheff, A. L. Lucius, S. B. Owens and G. M. Gray, *Organometallics*, 2011, **30**, 5695.
- 27 G. Weber, in *Molecular Biophysics*, ed. B. Pullman and M. Weissbluth, Academic Press, New York, New York, 1965.
- 28 N. L. Brennan, C. L. Barnes and E. Bosch, *Inorg. Chim. Acta*, 2010, **363**, 3987.
- 29 C. Hansch, A. Leo and R. W. Taft, *Chem. Rev.*, 1991, **91**, 165.
- 30 ApexII Suite, Bruker AXS Ltd., Madison, WI, 2006.
- 31 G. M. Sheldrick, *Acta Crystallogr., Sect. A: Fundam. Crystallogr.*, 2008, **64**, 112.
- 32 L. J. Barbour, *J. Supramol. Chem.*, 2001, **1**, 189.
- 33 <http://journals.iucr.org/services/cif/publicif/>